International Journal of Research and Review
[Indexed, Peer-Reviewed Journal]
Volume 12; Issue: 4; April 2025
Website: www.ijrrjournal.com
Research Paper *E-ISSN: 2349-9788; P-ISSN: 2454-2237*

Preparation of TiO_2 Nanoparticles Using Microwave and Techniques of Pulsed Laser Ablation and Their Properties

Luma H. Abed

Department of Basic Sciences, College of Dentistry, University AL-Qadisiyah, AL-Qadisiyah, IRAQ

Corresponding Author: Luma H. Abed

DOI: https://doi.org/10.52403/ijrr.20250439

ABSTRACT

This study presents an economical and swift approach for producing titanium dioxide (TiO2) nanoparticles through the integration of microwave irradiation and pulsed laser ablation techniques. Titanium isopropoxide (Ti [OCH(CH3)2]4) served as the precursor, whereas deionized water (DIW) functioned as both the solvent and reducing agent during the microwave synthesis procedure. The microwave-assisted synthesis entailed a 5-minute reaction at 1200 W in a commercial microwave, succeeded by annealing at 400°C for one hour. A Q-switched Nd: YAG laser, delivering 480 mJ per pulse, was employed for pulsed laser ablation in a liquid media, with pulse counts of 100, 200, and 300. Numerous analytical methods, such as X-ray diffraction, field-emission scanning electron microscopy, Fourier transform infrared spectroscopy, and assessment of antibacterial activity, were used to assess the generated nanoparticles. XRD examination verified the existence of anatase TiO2 in the nanoparticles created via microwave. Morphological investigation revealed that microwave-synthesized particles exhibited a combination of spherical and irregular morphologies with a uniform distribution, with average diameters of 52.707 nm, 65.602 nm, and 82.095 nm. Pulsed laser ablation, by contrast, yielded primarily spherical nanoparticles measuring between 50.81 nm and 71.22 nm. FTIR examination revealed an absorption peak at 733 cm^{-1}, indicative of Ti–O stretching vibrations in microwave-synthesized nanoparticles, but the pulsed laser ablation samples displayed a distinct Ti–O–Ti stretching vibration peak at 657 cm^{-1}. The antibacterial efficacy of the produced TiO2 nanoparticles was evaluated against Escherichia coli, Staphylococcus aureus, Klebsiella pneumoniae, and Pseudomonas aeruginosa, indicating their potential for antimicrobial applications.

Keywords: Nanoparticles, Titanium isopropoxide (TTIP), Laser ablation, Nd: YAG laser, titanium dioxide, surface area.

INTRODUCTION

Nanomaterials, defined by dimensions ranging from one to one hundred nanometers, exhibit distinctive qualities that position them at the forefront of cutting-edge technologies across diverse sectors [1]. Their superiority over conventional materials lies in enhanced mechanical, chemical, electrical, and thermal properties, including notable wear and corrosion resistance. Nanomaterials, being both lighter and stronger than traditional counterparts, find applications in pivotal industries such as electronics, healthcare, energy, environmental sciences, and materials research [2]. In the realm of electronics,

nanomaterials contribute to the development of flexible electronics, high-resolution screens, and compact electronic devices. Similarly, in the medical field, they play a crucial role in crafting specialized medications and miniature medical devices[3]. The selection of titanium dioxide (TiO2) as a research material is driven by its distinctive attributes, encompassing high permittivity, refractive index, efficiency, affordability, chemical inertness, non-toxicity, photocatalytic activity, photo stability, and the ability to degrade a wide range of organic molecules.TiO2, notable for its exceptionally high refractive index surpassed only by diamonds, unlocks novel applications in providing whiteness and opacity to diverse items such as paints, coatings, plastics, paper, fibers, food, and cosmetics. The existence of three crystalline polymorphs of TiO2, namely rutile and anatase in the tetragonal phase, and brookite in the orthorhombic phase, further accentuates its versatility and potential for varied applications [4].

MATERIALS & METHODS

Utilizing titanium (IV) isoprenoid (TTIP) and demineralised water (DMW) as solvents and decrease agents for the creation of sub-micrometer atoms, titanium dioxide (TiO2) powder was synthesized utilizing the microwave-assisted method. In a glass jar, 100 mL of DIW was forcefully magnetically swirled at 600 rpm for 10 minutes while 10 mL of TTIP was progressively introduced. A Sharp-38L microwave oven running at 2.45 GHz with power levels set at 40%, 60%, and 100% of 1200 W for five minutes was used to do the microwave synthesis. The formation of TiO2 nanoparticles was indicated by the solution turning milky white (Figure 1a). The precipitate was then rinsed with DIW and absolute ethanol before being centrifuged at 4500 rpm for 5 minutes (Figure 1b).

After centrifugation, the sample was dried in an oven at 60°C for one hour and left overnight. To improve its crystallinity, the dried powder was next calcined in air for an hour at 400°C in an ELF 11/14B furnace. (Figure1-c).

(a) (b) (c)

Fig. (1) Stages of Combine specimens
(a) The appearance of the solution after titration.
(b) The solid product after treatment with ethanol and water.
(c) The final appearance of the product after annealing at 400°C for 1 hour.

Laser ablation was employed for nanoparticle synthesis due to its simplicity and cost-effectiveness. The process involved immersing high-purity TiO_2 in double-distilled deionized water (DDDW) at room temperature. Initially, 5 grams of titanium dioxide (TiO_2) was compressed into a 2-centimeter mold for 15 minutes without the use of additional chemicals. The compressed TiO_2 was then placed at the base of a quartz container, and 4 mL of liquid was added.

The samples were exposed to a 1064 nm Q-switched Nd: YAG laser, with each laser

pulse lasting 7 nanoseconds and repeating at a frequency of 5 Hz. The laser energy for TiO_2 ablation was set at 480 millijoules per pulse. The compressed TiO_2 was subjected to 100, 200, and 300 laser pulses.

Focusing the laser beam on the TiO_2 nanostructure led to high-energy surface interactions, inducing the formation of surface plasmons—electromagnetic oscillations caused by variations in electron density. These plasmons influence chemical reactions and facilitate the diffusion of TiO_2 atoms. A 100-mm focusing lens was used to direct the laser beam onto the TiO_2 target, ensuring precise energy delivery for effective nanoparticle synthesis.

RESULT AND DISCUSSION

X-ray Diffraction

The (XRD) forms of the produced TiO_2 nanoparticle samples are shown in Figure 2. The development of high crystallinity nanomaterials is confirmed by the diffraction peaks. The JCPDS file No. 21-1272 indicates that the produced TiO_2 nanoparticles are mainly found in the anatase phase, which is supported by the XRD study. The tetragonal structure of anatase TiO_2 is shown by a strong (101) peak in the diffraction patterns at about $2\theta = 25.33^{o}$. The interaxial angles are $\alpha = \beta = \gamma = 90°$, and the computed lattice parameters are b = a = 0.37852 nm, c = 0.65139 nm. The great purity of the manufactured TiO_2 nanoparticles is indicated by the lack of peaks that correspond to other phases or contaminants. By examining the expansion of anatase TiO2 peaks at various 2θ values, the Debye-Scherrer equation was used to estimate the average crystalline size of the TiO2 nanoparticles [5]. As shown in Table 1, The produced nanoparticles' crystalline sizes range from 3.73 nm to 8.46 nm, according to the data. The uniform heating mechanism of the microwave-assisted synthesis contributed to the homogeneous heating of the TiO2 material, facilitating the rapid formation of the anatase phase within a short processing time [6–7].

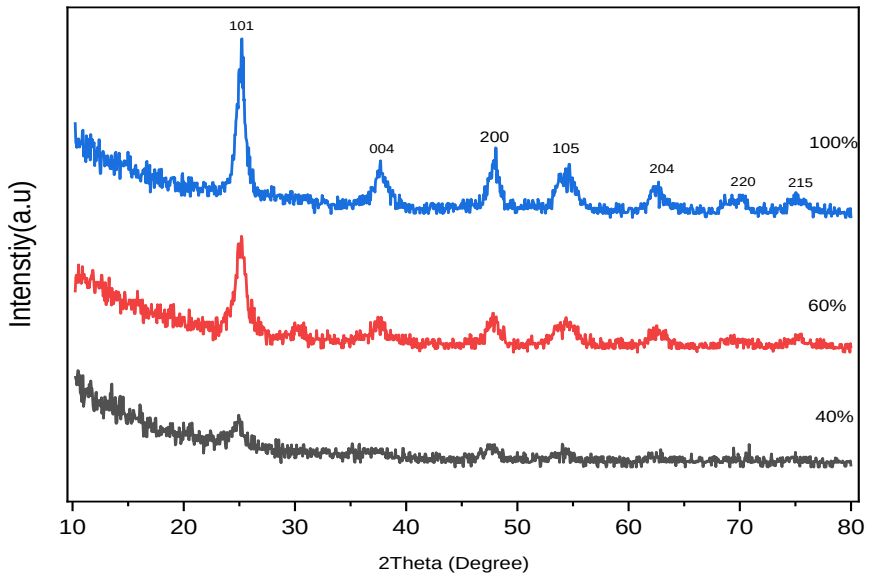

Fig. (2) X-ray diffract grams of the TiO2 Nanoparticles.

Table (1) The synthesized TiO2 nanoparticles' average crystallite diameters.

microwave power	Average crystallite size (D) (nm)
40%	3.73
60%	5.98
100%	8.46

Figure 3 illustrates the X-ray diffraction (XRD) patterns of the TiO_2 nanoparticles synthesized via pulsed laser ablation. The diffraction peaks confirm the formation of nanomaterials with significant crystallinity. Based on the XRD analysis, the synthesized TiO_2 nanoparticles predominantly exist in the brookite phase, as identified by JCPDS file No. 29-1360.A distinct (120) peak is observed at approximately 2θ = 25.33º, which corresponds to the rhombohedral structure of brookite TiO_2. The calculated lattice parameters for this phase are a = b = c = 0.37852 nm, with interaxial angles α = β = γ ≤ 90°.Table 3 Give a brief overview of the TiO_2 nanopowders' XRD data after they were created using pulsed laser ablation. As shown in Table 2, the average crystalline size of the prepared samples ranges from 3.30 nm to 2.31 nm, indicating the formation of ultra-small TiO_2 nanoparticles.

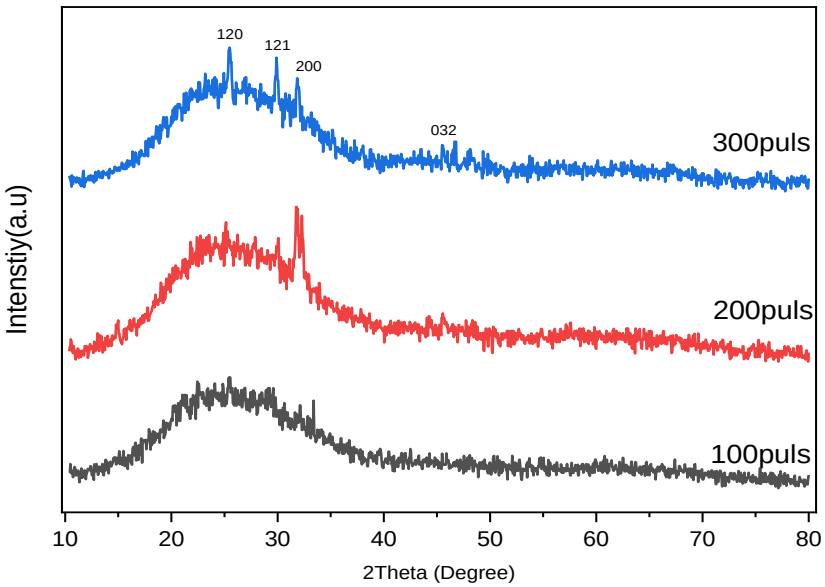

Fig. (3) X-ray Using the laser ablation process, scatter grams of TiO2 nanoparticles.

Table (2) Average crystallite sizes of the TiO2 nanoparticles produced using the laser ablation technique.

Laser pulse	Average crystallite size (D) (nm)
100puls	3.30
200puls	3.03
300puls	2.31

Field-emission scanning electron microscopy (FESEM)

Figures 4, 5, and 6 show the surface morphology of the produced TiO_2 specimens as determined by field-emission scanning electron microscopy (FESEM). The FESEM images for samples synthesized at 40%, 60%, and 100% power levels reveal a distribution of spherical particles. These spherical clusters are dispersed across different regions, with average diameters of 52.707 nm, 65.602 nm, and 82.095 nm, respectively, corresponding to rising energy levels. A deeper look at the FESEM pictures reveals a rough surface texture and large pore diameters, which contribute to the high specific surface area in all three cases. Figures 7, 8, and 9 present the FESEM images of the samples synthesized using 100, 200, and 300 laser pulses. The observed particles exhibit a combination of spherical and irregular

shapes, with a consistent distribution. These particles appear either as individual entities or as clusters. The measured average particle sizes are 50.81 nm, 62.33 nm, and 73.22 nm for the samples subjected to 100, 200, and 300 laser pulses, respectively.

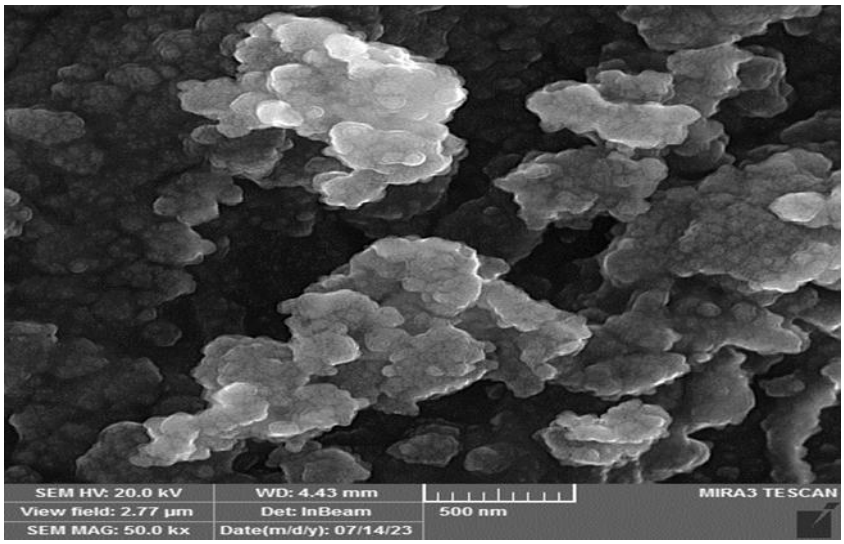

Fig. (4) FESEM images of TiO2 Nanoparticles at 40%.

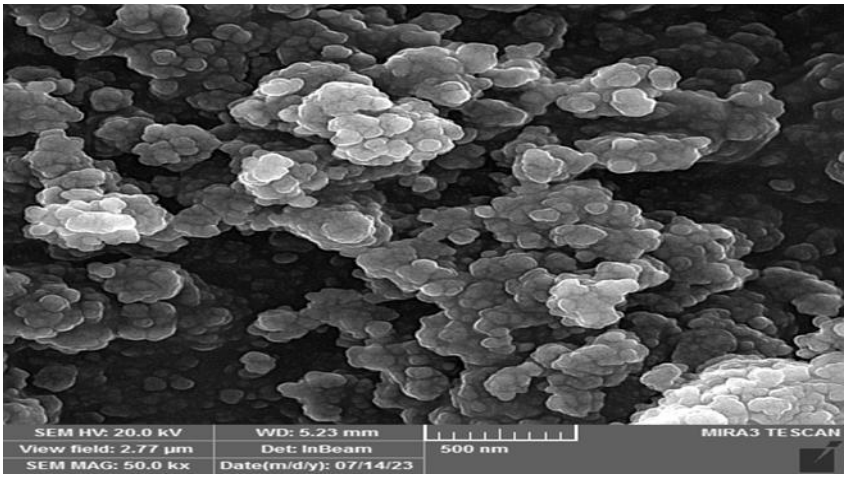

Fig. (5) FESEM images of TiO2 Nanoparticles at 60%.

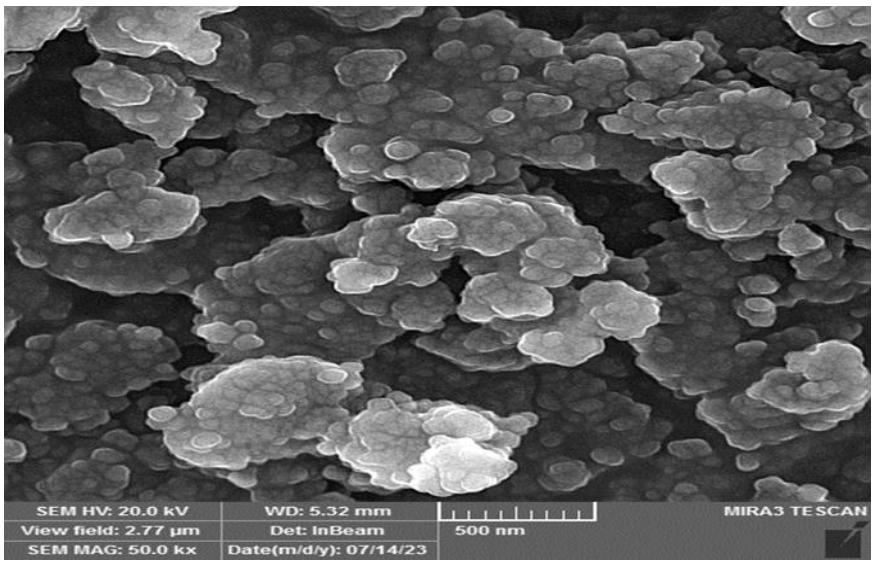

Fig. (6) FESEM images of TiO2 Nanoparticles at 100%.

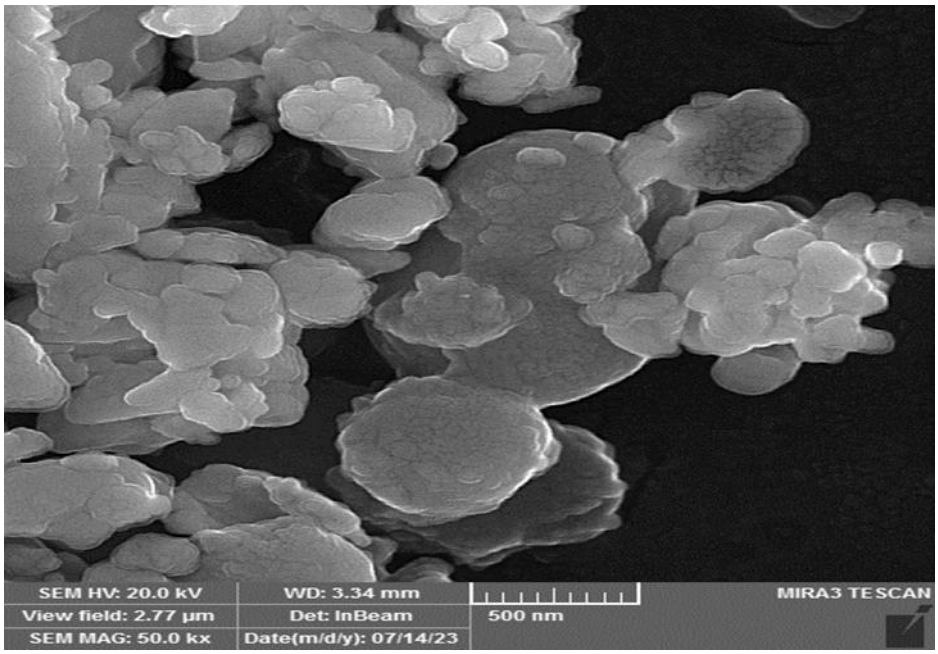

Fig. (7) FESEM images of TiO2 nanoparticles prepared by laser ablation method at 100puls.

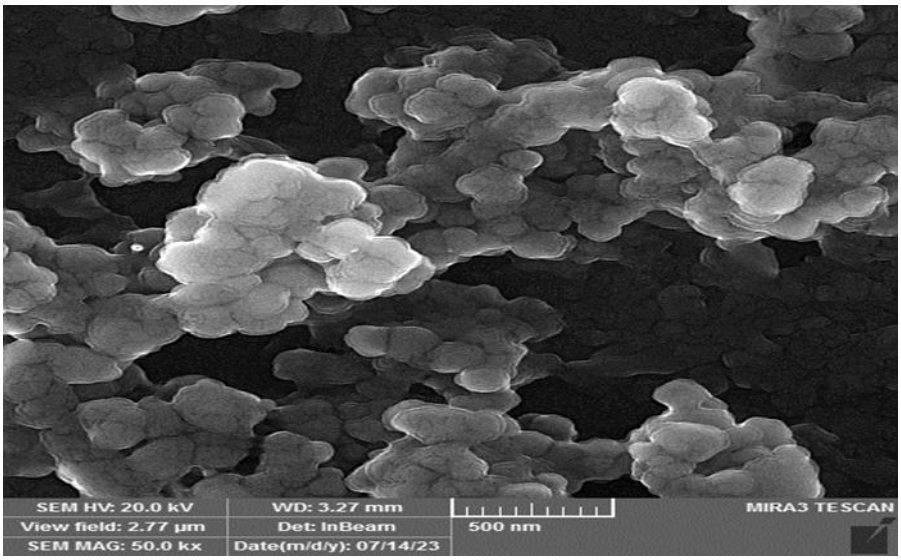

Fig. (8) FESEM images of TiO2 nanoparticles prepared by laser ablation method at 200puls.

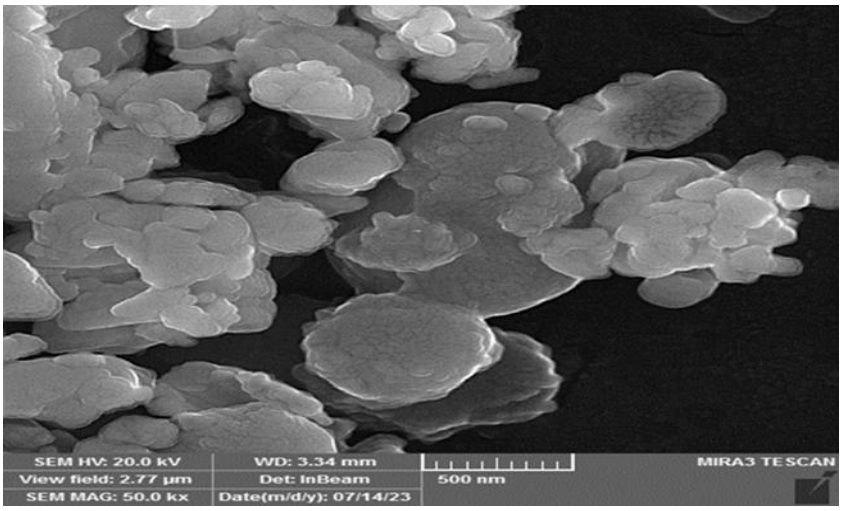

Fig. (9) FESEM pictures of TiO2 nanoparticles made at 300 puls using the laser ablation technique.

FTIR spectrum

Figure 10 displays the FTIR spectrum of the TiO2 nanoparticles produced using a microwave technique. The band stretching motion of the O-H moiety at (3789-3422) cm-1, which is brought on by the physisorption of water and reveals the moisture content in the samples, was connected to the broad absorption band at (3300-3800) cm-1 [8,9]. The non asymmetric stretching of the CH3 end groups of the alkyl chain is responsible for the peak at 2916 cm-1 [10]. Because of the chemically absorbed water in the solution, the weak bands at 1623 cm-1 and 1111 cm-1 are attributed to O-H bending groups [10]. The unique vibrations of the inorganic Ti-O-Ti stretching in titanium dioxide (TiO2) are seen in the IR spectrum in the absorption area below 950 cm-1. The peak at 733.32 cm-1 in the anatase stage was found to be caused by Ti-O-Ti stretching vibrations, indicating that the intense absorption of titanium dioxide caused by Ti-O stretching transformed into Ti-O-Ti bridge stretching or bending vibrations [11].

Figure 11 shows the FTIR spectrum that was acquired from the TiO2 the nanoparticles produced by laser ablation display displayed optical characteristics. The broad absorption band observed between 3300 and 3800 cm-1 is caused by the stretching vibration of the hydroxyl O-H group at 3500 cm-1. This vibration, which is caused by the physical absorption of water, shows that there is moisture in the samples. The faint bands at 2060 cm-1 and 1630 cm-1 are caused by water in solution that has been chemically absorbed by O-H bending groups. The Ti-O-Ti stretching vibrations were identified as the cause of the peak at 657 cm-1. which indicated that titanium dioxide absorbed a significant amount of energy as a result of Ti-O bridge stretching or bending vibration rather than Ti-O stretching.

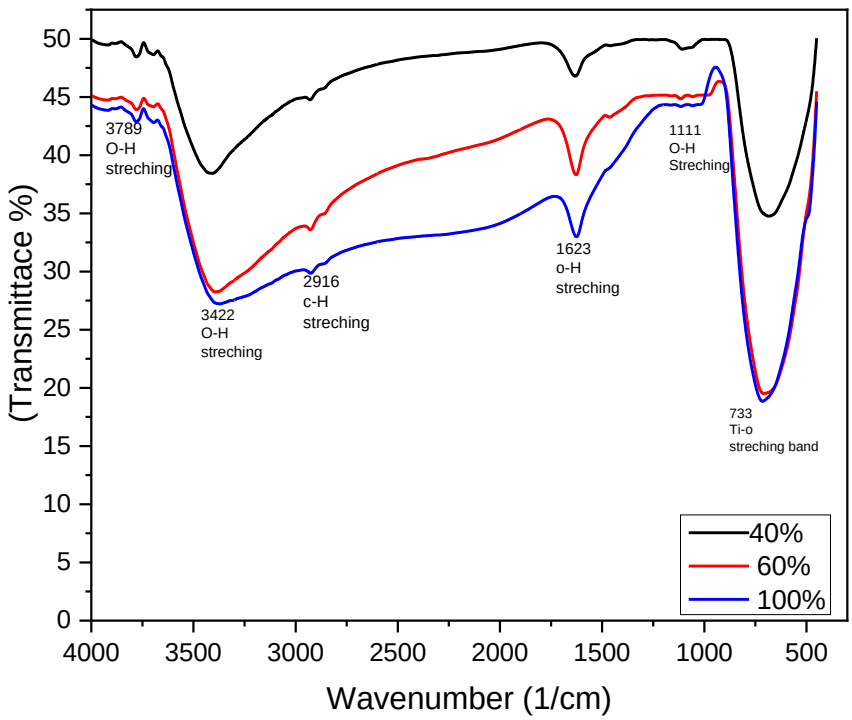

Fig. (10) FTIR spectrum of TiO2 nanoparticles prepared by microwave method.

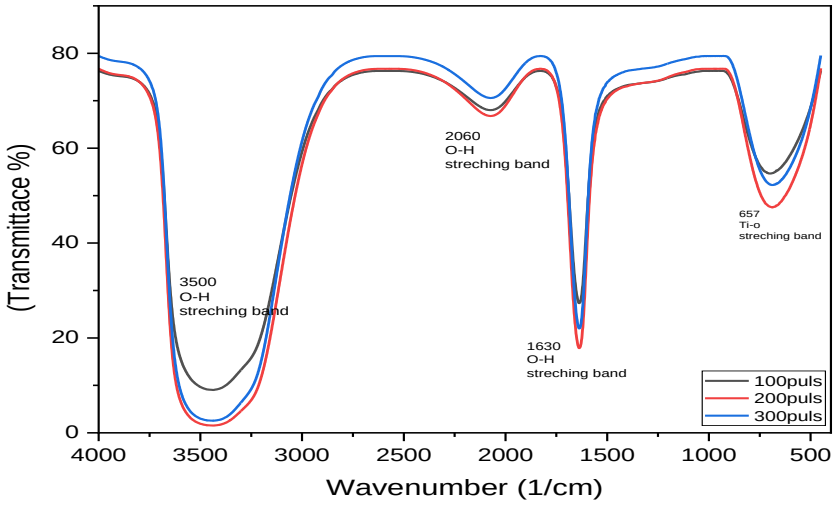

Fig. (11) TiO2 nanoparticles generated by laser ablation at 100, 200, and 300 puls have an FTIR spectrum.

Antibacterial activity

TiO2 NPs' antibacterial activity was tested against microorganisms such as Escherichia coli, Staphylococcus aureus, Klebsiella pneumonia, and Pseudomonas aeruginosa. TiO2 nanoparticles are (40%, 60%, and 100%) samples by microwave method and (100puls, 200puls, 300puls) samples by laser ablation method, as indicated in Table (3). As seen in Figure (12), the bacterial inhibition zone's maximum value occurs at 100% power. The samples (60%) and (100%) in (Bet) clearly have a bigger surface area. The bacterial inhibition zone may expand as a result of the catalytic nanomaterial's larger surface area.

Table (3) shows the antibacterial activity of TiO2 NPs using the microwave technique.

Bacterial isolate	***E. coli inhibition zone(mm)***		***S. aureus inhibition zone(mm)***		***K. pneumoniae inhibition zone(mm)***		***P. aeruginosa inhibition zone(mm)***	
40%	4	R	3	R	2	R	2	R
60%	6	M	6	M	5	M	5	M
100%	10	S	11	S	9	S	10	S

R=Resistant less than 5 mm
S=Sensitive more than 10mm
M=Moderate from 5 to 10 mm

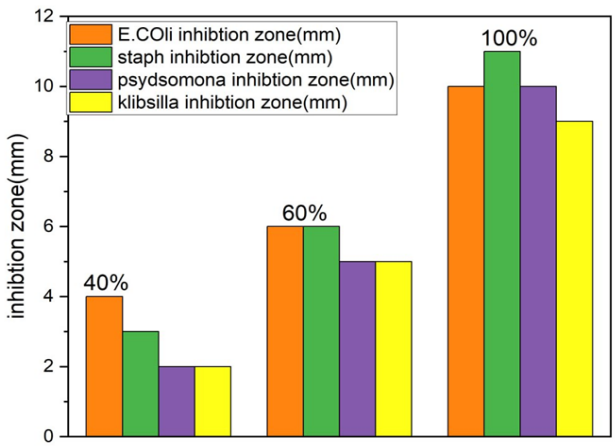

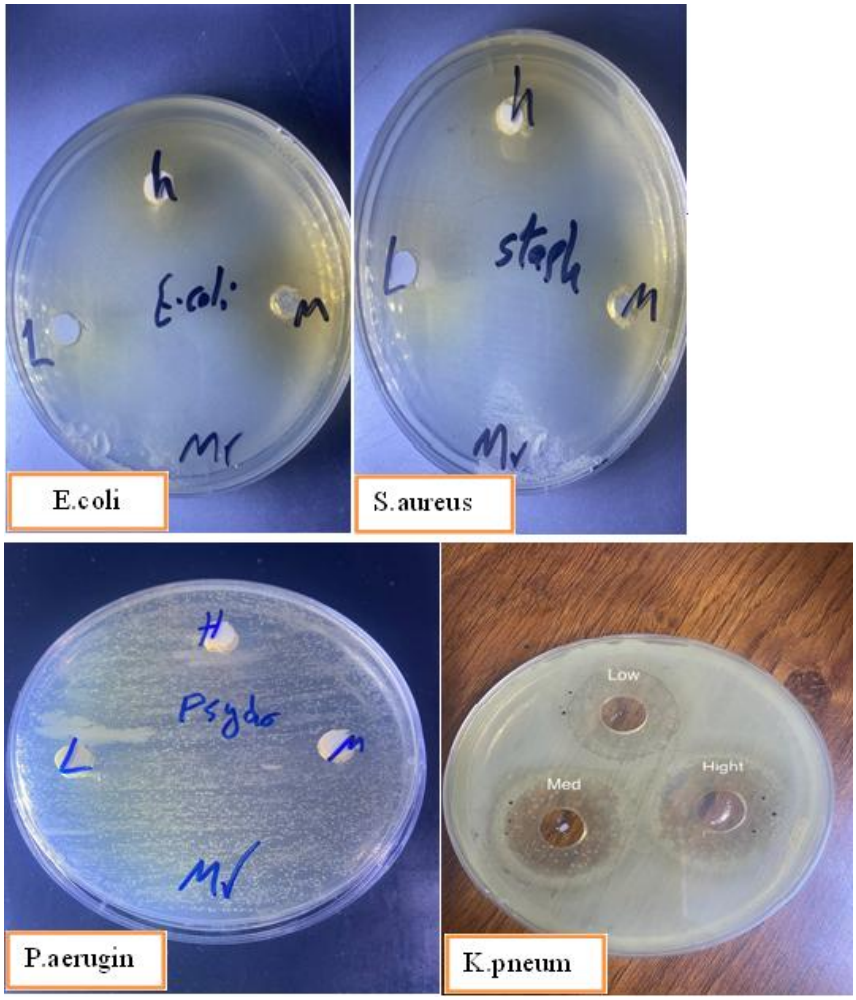

Figure (12) Image of inhibition zone of bacteria by microwave method.

TiO_2 nanoparticles shown antibacterial efficacy against Escherichia coli, Staphylococcus aureus, Klebsiella pneumoniae, and Pseudomonas aeruginosa (see Table 4). The data in Figure 12 show that the maximum bacterial inhibition zone was observed at 300 pulses. Notably, samples produced at 200 and 300 pulses have a larger surface area, as determined by Brunauer-Emmett-Teller (BET). The increased surface area of the catalytic nanomaterial is most likely responsible for the increased bacterial inhibition, as a bigger surface area allows for more interaction with bacterial cells, boosting antimicrobial efficacy.

Table (4): Antibacterial activity of TiO2 NPs by laser ablation method.

Bacterial isolate	***E.coli inhibition zone(mm)***		***S.aureus inhibition zone(mm)***		***K.pneumoniae inhibition zone(mm)***		***P.aeruginosa inhibition zone(mm)***	
100 puls	2	R	3	R	1	R	1	R
200 puls	4	R	4	R	3	R	5	R
300 puls	8	M	8	M	6	M	7	M

R=Resistant less than 5 mm
S=Sensitive more than 10mm
M=Moderate from 5 to 10 mm

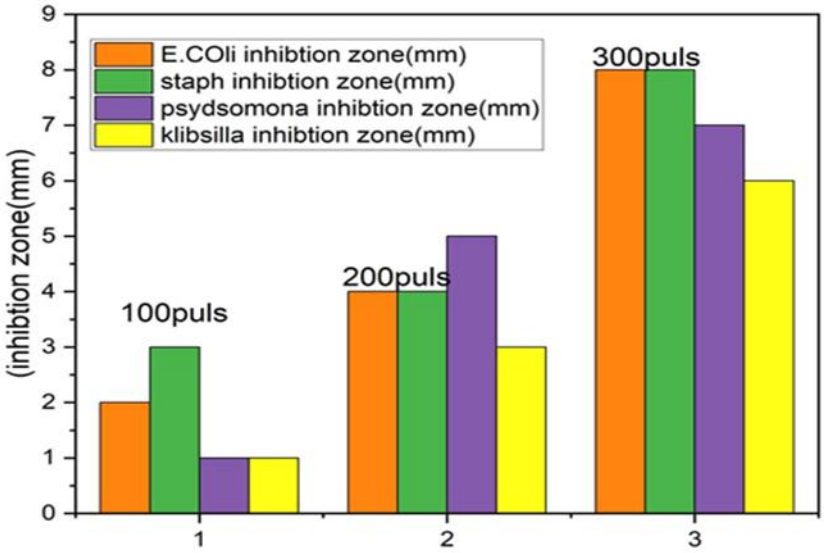

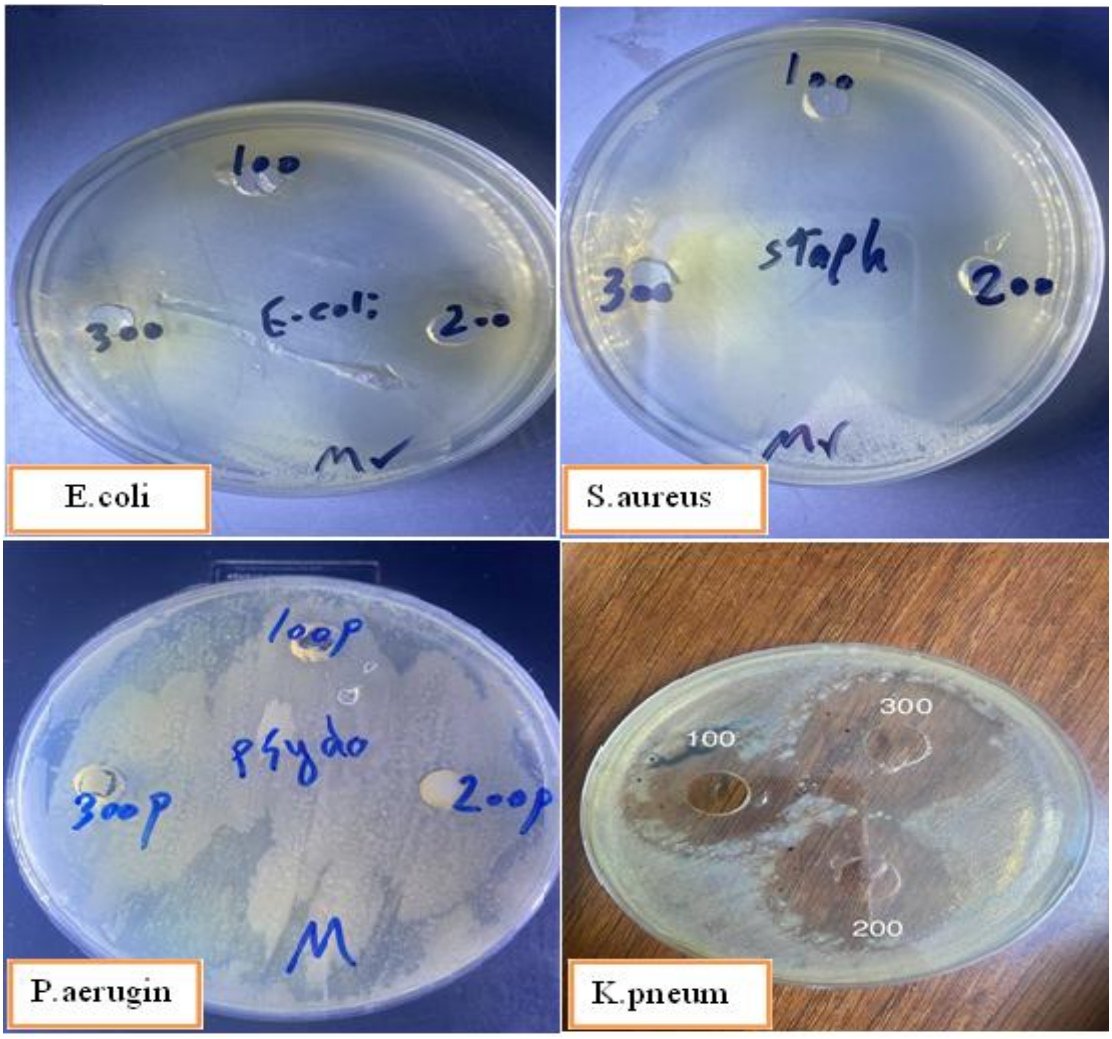

Figure (13) Image of inhibition zone of bacteria by laser ablation method.

CONCLUSION

This study found that integrating microwave technology with pulsed laser ablation offers a quick, efficient, and simple way to synthesize TiO_2 nanoparticles. X-ray diffraction (XRD) investigation confirms TiO_2 nanoparticles generated via microwave-assisted synthesis exist in the

anatase phase, with a clear (101) peak at roughly 2θ = 25.28º. The absence of extra peaks in the XRD patterns emphasizes the samples' exceptional purity. In contrast, the TiO_2 nanoparticles created using pulsed laser ablation were discovered to be in the brookite phase. FESEM examination showed that microwave-synthesized TiO_2 samples had average particle sizes ranging from 52.707 nm to 82.095 nm, while laser ablation samples varied from 50.81 nm to 71.22 nm. FTIR spectroscopy revealed Ti-O-Ti stretching vibrations in microwave-synthesized TiO_2 samples, with absorption bands below 950 cm^{-1}. Laser ablation-synthesized TiO_2 samples showed a distinct absorption peak at 657 cm^{-1}. Antibacterial activity tests revealed the maximum inhibition efficiency of 100% for the microwave-created sample at full power and the pulsed laser ablation sample synthesized with 300 pulses.

Declaration by Authors

Ethical Approval: Not applicable

Acknowledgement: None

Source of Funding: None

Conflict of Interest: No conflicts of interest declared.

REFERENCES

1. Baig, Nadeem, Irshad Kammakakam, and Wail Falath. "Nanomaterials: A review of synthesis methods, properties, recent progress, and challenges." Materials Advances (2021) ,1821-1871 :2.6
2. KUMAR, Naveen; MAITI, Nandita; THOMAS, Susy. Insights into Plasmon-Induced Dimerization of Rhodanine–A Surface-Enhanced Raman Scattering Study. The Journal of Physical Chemistry, (2023).
3. ZHANG, Shuai, et al. Advanced titanium dioxide-polytetrafluorethylene (TiO2-PTFE) nanocomposite coatings on stainless steel surfaces with antibacterial and anti-corrosion properties. Applied Surface Science (2019),490:231-241.
4. AL-KAISY, Hanaa A., et al. Preparation and Characterization of TiO2-ZrO2 Coating Prepared by Sol-Gel Spin Method. THE IRAQI JOURNAL FOR MECHANICAL AND MATERIALS ENGINEERING,20.3: 257-267, (2020).
5. Barnard AS, Zapol P, Curtiss LA. Modeling the morphology and phase stability of TiO2 nanocrystals in water. J Chem Theory Compute. 2005;1(1):107-16.
6. Mute DK, Deena BF. The effect of tetra isopropyl orthotitanate (TIP) concentration on structural, and luminescence properties of titanium dioxide nanoparticles prepared by sol-gel method. Mater Sci Semi Cond Process. 2020;10(6):104-783.
7. Reda S. Jalawkhan, Firas K. Mohamed Alosfur,Ahmed M. Abdul-Lettif. "Characterization of pure anatase TiO2 nano rods synthesized by microwave method", AIP Publishing, 2022.
8. Hindy A, Farahmand F, Pourdanesh F, Torshabi M, Al Janabi AH, Rasoulianboroujeni M, et al. Synthesis and characterization of 3D-printed functionally graded porous titanium alloy. J Mater Sci. 2020;55(21):9082–94.
9. Brantley SL, Mellott NP. Surface area and porosity of primary silicate minerals. Am Mineral. 2000;85(11–12):1767–83.
10. Hassan SA, Raheem, Salman JA, Sattar A-J, Sajid S. Characterization of Titanium dioxide (TiO2) Nanoparticles Biosynthesized using Leuconostoc spp. Isolated from Cow's Raw Milk: Characterization of (TiO2) Nanoparticles. Proceedings of the Pakistan Academy of Sciences: B Life and Environmental Sciences. 2023;133–42.
11. Fathy M, Hamad H. Influence of calcination temperatures on the formation of anatase TiO2 nanorods with a polyol-mediated solvothermal method. RSC Advances. 2021;6(9):7310.

How to cite this article: Luma H. Abed. Preparation of TiO_2 nanoparticles using microwave and techniques of pulsed laser ablation and their properties. *International Journal of Research and Review*. 2025; 12(4): 316-326. DOI: *10.52403/ijrr.20250439*

******